Technologies and Materials for Renewable Energy, Environment & Sustainability

Electrical and Structural Characteristics of the Sol-Gel-Prepared HgBa2Ca2Cu3O8+δ Superconductor at Various Sintering Temperatures

AIPCP25-CF-TMREES2025-00017 | Article

Submitted on: 11-12-2025

Electrical and Structural Characteristics of the Sol-Gel-Prepared $HgBa_2Ca_2Cu_3O_{8+\delta}$ Superconductor at Various Sintering Temperatures

Ahmed Majid Safi[1, a)] and Sabah Jalal Fathi[1, b)]

Department of Physics, College of Education for Pure Science, University of Kirkuk, Kirkuk, Iraq

[a)] *Corresponding author: mr.ahmed521h@gmail.com*
[b)] *prof.sabahjalal@uokirkuk.edu.iq*

Abstract: In this study, high-temperature superconducting samples of $HgBa_2Ca_2Cu_3O_{8+\delta}$ (Hg-1223) were synthesized using the Sol-Gel method and sintered at three different temperatures: 800°C, 825°C, and 850°C. Structural characterization using X-ray diffraction (XRD) confirmed the formation of the desired Hg-1223 phase, with varying degrees of phase purity depending on the sintering temperature. Lattice parameters, phase ratios, and crystallite sizes were calculated and correlated with the processing conditions. Surface morphology examined by scanning electron microscopy (SEM) at 5 μm magnification revealed clear grain growth and increased densification with rising sintering temperatures. The microstructural evolution contributed significantly to the electrical behavior of the samples. Electrical resistivity measurements as a function of temperature showed superconducting transitions in all samples with a constant onset critical temperature ($T_{c(onset)} \approx 171.3$ K). The sample sintered at 850°C exhibited the sharpest transition ($\Delta T_c \approx 37.3$ K), indicating improved homogeneity and stronger intergranular connectivity. All samples displayed comparable energy gap values (~0.026 eV), confirming the superconducting nature of the Hg-1223 phase. Overall, the results demonstrate that the Sol-Gel method is an effective route for producing high-quality Hg-based superconductors. The sample processed at 850°C achieved the best combination of structural integrity, phase purity, and superconducting performance, making it a promising candidate for future applications in high-temperature superconducting technologies.

Keywords: superconducting; sol–gel method; structural properties; thermal properties; electrical properties

INTRODUCTION

Superconductivity is one of the most important physical phenomena in solid-state physics, characterized by the complete loss of electrical resistance in certain materials when cooled below a critical temperature (T_c) [1]. Among the various families of superconducting materials, layered copper-based compounds (cuprates) have received considerable attention, particularly mercury-based high-T_c superconductors, due to their relatively high transition temperatures and exceptional electronic properties [2, 3]. The compound $HgBa_2Ca_2Cu_3O_{8+\delta}$ (commonly referred to as Hg-1223) is considered one of the most promising members of the mercury-based superconductor family, as it exhibits a critical temperature exceeding 130 K [4, 5]. This makes it a strong candidate for advanced technological applications such as magnetic sensors, superconducting power transmission, and high-efficiency electronic devices [6]. However, synthesizing this compound poses several challenges, including mercury volatility at high temperatures and the difficulty of stabilizing the desired superconducting phase [7]. To overcome these limitations, several synthesis methods have been developed.

among which the sol-gel method stands out as an effective wet-chemical technique for producing highly homogeneous nanostructured powders. This method enables better atomic-scale distribution of the constituent elements and allows for lower sintering temperatures, which in turn improve both structural and electrical properties of the resulting samples [8, 9].

In this study, the $HgBa_2Ca_2Cu_3O_{8+\delta}$ compound was prepared using the sol-gel technique, and the effects of **different** sintering temperatures (800°C, 825°C, and 850°C) on its structural and electrical properties were investigated. The study includes X-ray diffraction (XRD) analysis for phase identification, atomic force microscopy (AFM) for surface morphology examination, and electrical resistivity measurements as a function of temperature to determine the superconducting transition temperatures of the prepared samples.

EXPERIMENTAL PROCEDURE

The $HgBa_2Ca_2Cu_3O_{8+\delta}$ superconducting compound was synthesized using the sol-gel method. High-purity nitrates of mercury [$Hg_2(NO_3)_2 \cdot 2H_2O$], barium $Ba(NO_3)_2$, calcium $Ca(NO_3)_2 \cdot 4H_2O$, and copper $Cu(NO_3)_2 \cdot 3H_2O$ were used as starting materials. The required stoichiometric ratios were calculated based on atomic weight, and precise quantities were weighed using a high-sensitivity electronic balance (KERN) [10].

Each nitrate was dissolved separately in distilled water under magnetic stirring. For mercury nitrate, a small amount of nitric acid (HNO_3) was added to prevent precipitation. The solutions were combined gradually under controlled stirring at 65°C to form a uniform acidic solution (pH ≈ 1). To initiate gelation, approximately 4 ml of ammonia (NH_3) was added, leading to an increase in viscosity and pH (≈ 4), and resulting in the formation of a light blue gel [11, 12].

The gel was poured into a ceramic crucible and left to rest at room temperature before drying. It was then heat-treated at 200°C, 225°C, and finally 250°C for a total of four hours to remove excess water and volatile components. The dried product was ground into a fine powder using a mortar and pestle with isopropanol drops to prevent scattering [13, 14]

A preliminary calcination step was conducted at 600°C for 8 hours (heating rate 5°C/min) to decompose residual nitrates and promote the initial formation of the compound. After cooling, the powder was reground and pressed into disc-shaped pellets (~2 g each, 18 mm diameter, ~1.9 mm thickness) using a hydraulic press under 7 ton/cm^2 pressure [15. 16].

Finally, the pellets were sintered at different temperatures (800°C, 825°C, and 850°C) for 10 hours, followed by controlled cooling. The resulting samples were dense, crack-free, mechanically stable, and ready for structural and electrical characterization [17].

RESULTS AND DISCUSSION

This section presents and discusses the key scientific findings related to the structural, morphological, and electrical properties of the $HgBa_2Ca_2Cu_3O_{8+\delta}$ superconducting samples synthesized via the sol–gel method. The influence of sintering temperature on phase formation and crystallographic behavior was examined using X-ray diffraction (XRD), which provided detailed information on phase composition, crystal structure, and phase purity [18]. The high-temperature superconducting phase (Hg-1223) was identified, and its volume fraction (HTP%) was calculated using relative peak intensities. Lattice parameters (a, b, c), unit cell volume (V), c/a ratio, and theoretical density were determined to assess structural changes. Crystallite size was also estimated using Scherrer's equation to evaluate the effect of thermal processing on grain refinement and crystallinity [19, 20].

The surface morphology of the samples was investigated using scanning electron microscopy (SEM), revealing the grain connectivity, size distribution, and uniformity, factors that play a crucial role in determining the current-carrying capacity and overall superconducting performance [21, 22].

Furthermore, the electrical resistivity of the samples was measured as a function of temperature (R–T) to determine the superconducting transition temperature (T_c) and analyze the effect of sintering temperature on the transport properties of the Hg-1223 phase. This correlation between structural, microstructural, and electrical characteristics provides a comprehensive understanding of the optimal processing conditions required for high-performance superconductors prepared via the sol–gel technique.

STUDY OF STRUCTURAL PROPERTIES

XRD analysis

X-ray diffraction (XRD) analysis was conducted on the samples sintered at 800°C, 825°C, and 850°C to examine the formation of the high-temperature superconducting phase $HgBa_2Ca_2Cu_3O_{8+\delta}$ (Hg-1223) and to detect any secondary phases such as Hg-1201 and $CaHgO_2$. The diffraction patterns revealed distinct variations in phase purity and crystallographic properties depending on the sintering temperature [23].To quantitatively determine the volume fraction of the high-temperature superconducting phase (HTP%), the intensity of the characteristic peaks of the Hg-1223 phase was compared to the total intensity of all detected peaks using the following equation [24]:

$$HTP\% = \frac{\sum I_{Hg-1223}}{\sum I_{all\ phases}} \times 100\% \quad (1)$$

Where $\sum I_{Hg\text{-}1223}$ is the summed intensity of the main diffraction peaks corresponding to the Hg-1223 phase, and $\sum I_{all\ phases}$ is the total intensity of all peaks present in the XRD pattern.

In addition, the average crystallite size of the samples was estimated using the Scherrer equation [25], which is given by

$$D = \frac{k\lambda}{\beta \cos\theta} \quad (2)$$

Here, D is the crystallite size, K is the shape factor (typically 0.9), λ is the wavelength of the X-ray radiation (1.5406 Å for Cu-Kα), β is the full width at half maximum (FWHM) of the diffraction peak in radians, and θ is the Bragg angle.

Fig. 1 presents the X-ray diffraction (XRD) patterns of $HgBa_2Ca_2Cu_3O_{8+\delta}$ samples synthesized via the sol–gel method and sintered at 800, 825, and 850°C, illustrating the influence of sintering temperature on phase purity and structural quality. At 800°C, the pattern is characterized by sharp and well-defined peaks corresponding to the Hg-1223 phase, with a noticeable suppression of secondary phases (Hg-1201 and $CaHgO_2$), reflecting high crystallinity and phase purity. The high-T_c phase percentage (HTP%) reached 66.97%, the highest among the three samples, while the c/a ratio (4.0550) and c-lattice parameter (15.5273 Å) were close to the ideal values for a stable Hg-1223 crystal structure.

Upon increasing the temperature to 825°C, a reduction in the intensity of the Hg-1223 peaks was observed, accompanied by a significant increase in secondary phase peaks (* and ▲), indicating partial degradation or structural distortion due to exceeding the optimal sintering temperature. The HTP% decreased to 55.78%, and the c/a ratio dropped to 4.0076, suggesting possible lattice distortion or phase instability [25].

At 850°C, the pattern showed a partial recovery of the Hg-1223 peaks and a relative reduction in the intensity of the secondary phases compared to the 825°C sample; however, the crystallinity remained lower than that of the 800°C sample. The HTP% reached 60.88%, and the c-lattice parameter increased to 15.7516 Å, which could be attributed to oxygen uptake or partial structural transformation. Overall, 800°C proved to be the most favourable temperature for obtaining a pure and highly crystalline Hg-1223 phase using the sol–gel method, compared to 825°C and 850°C.

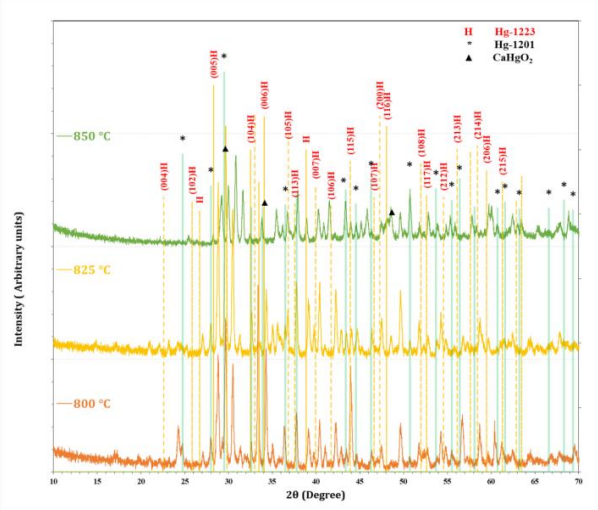

Fig. 1. X-ray diffraction patterns of $HgBa_2Ca_2Cu_3O_{8+\delta}$ samples prepared by the sol–gel method and sintered at 800, 825, and 850°C, showing the main Hg-1223 phase (H) and secondary phases Hg-1201 (*) and $CaHgO_2$ (▲).

Lattice Parameters, Phase Percentages, and Density

The structural parameters, calculated lattice constants, unit cell volumes, molar weights, theoretical densities, and phase ratios for the three samples are summarized in the following table:

Based on the XRD analysis, the sample sintered at 800°C exhibited the highest structural quality and phase purity, confirming that this temperature represents the optimal sintering condition for achieving a well-crystallized Hg-1223 phase using the sol-gel technique [26].

Table 1. Represents the values of X-ray constants a, b, c, Volume V, c/a, lattice mass W, mass density ρ_m, and volume fraction of the phase for the $HgBa_2Ca_2Cu_3O_{8+\delta}$ compound.

T (°C)	a (Å)	b (Å)	c (Å)	V ($Å^3$)	c/a	w (g/mole)	ρ_m (g/cm^3)	HTP %	LTP %
800	3.8292	3.9180	15.5273	232.955	4.0550	874.033	6.2294	66.97%	33.03%
825	3.8292	3.9013	15.4906	231.412	4.0076	874.033	6.2709	55.78%	44.22%
850	3.8239	3.9913	15.7516	240.407	4.0310	874.033	6.0363	60.88%	39.12%

SEM Analysis

The surface morphology of the $HgBa_2Ca_2Cu_3O_{8+\delta}$ samples sintered at 800˚C, 825˚C, and 850˚C was investigated using Scanning Electron Microscopy (SEM). All images were captured at a magnification of 5 µm, which allows for accurate observation of the grain size, distribution, and surface texture developed through the sol-gel synthesis route.

Sample Sintered at 800˚C

As shown in Fig. 2, the SEM image of the sample sintered at 800˚C reveals an ultra-fine, nearly nanometric grain structure. The grains appear densely packed and uniformly distributed, with no visible large pores or cracks. This dense and smooth microstructure is a characteristic result of the sol-gel method, which enables precise control over material homogeneity at the molecular level. The close packing of the grains, even at a relatively low sintering temperature, indicates the effectiveness of the method in promoting structural uniformity and low porosity. A few slight agglomerations are visible; however, the overall grain size remains small and evenly distributed, suggesting an early-stage but efficient sintering process [27].

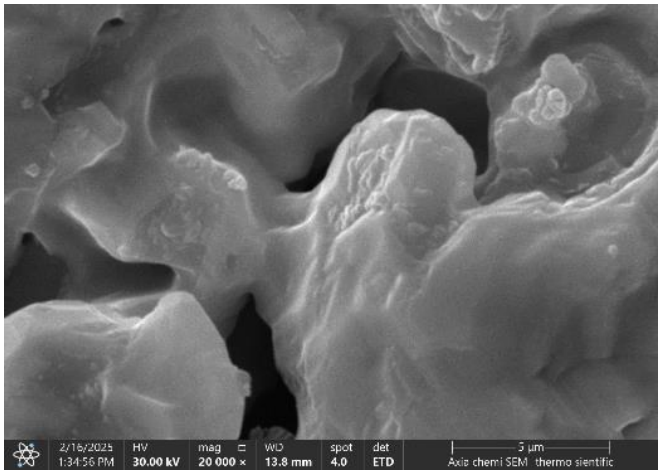

Fig. 2. SEM image of the sample sintered at 800°C (magnification: 5 µm)

Sample Sintered at 825˚C

The SEM image in Fig. 3 illustrates further development in the grain morphology. The grains become more defined and begin to show clearer boundaries, indicating improved crystallinity and grain bonding. The structure becomes more compact, with reduced micro-porosity compared to the 800˚C sample. This temperature appears to

mark a transition stage where the sintering process enhances both grain connectivity and densification, without compromising the fine grain size. No major surface defects or cracks are observed, reflecting structural stability and uniform thermal distribution during sintering [28]

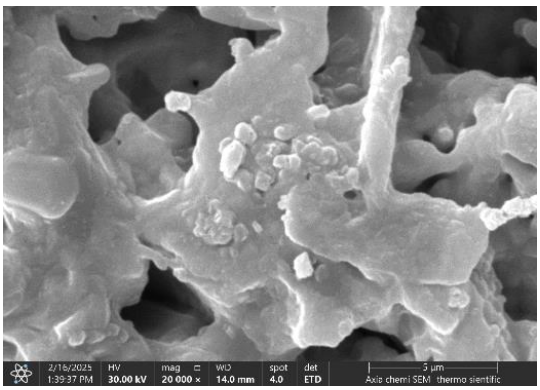

Fig. 3. SEM image of the sample sintered at 825°C (magnification: 5 µm)

Sample Sintered at 850°C

In Fig. 4. the SEM image of the sample sintered at 850°C shows a further increase in grain size, yet the distribution remains relatively uniform. The surface morphology appears denser and more consolidated, with a near-complete elimination of pores. The visible grain fusion and the formation of interconnected crystalline regions indicate advanced sintering and high structural coherence [29]. No significant cracks or morphological defects are observed. This sample exhibits the most compact and homogenous structure among the three, suggesting that 850°C represents an optimal condition for enhancing microstructural quality in sol-gel derived $HgBa_2Ca_2Cu_3O_{8+\delta}$.

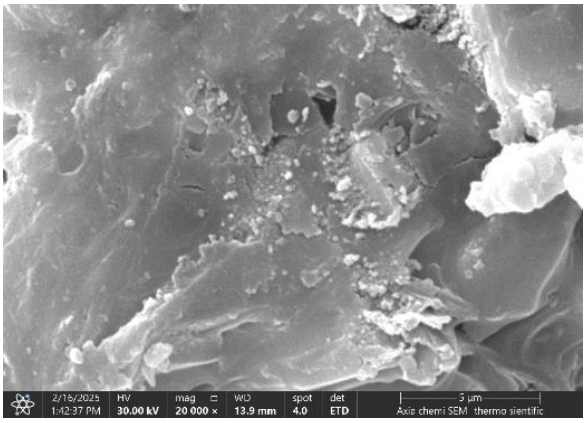

Fig. 4. SEM image of the sample sintered at 850°C (magnification: 5 µm)

Summary

Overall, the SEM analysis demonstrates a progressive improvement in grain connectivity, size uniformity, and surface density with increasing sintering temperature. The images captured at 5 µm magnification effectively illustrate microstructural evolution, confirming the efficiency of the sol-gel method in producing high-quality superconducting ceramics [30].

Electrical Resistivity Analysis

The temperature dependence of the electrical resistivity was investigated for all samples synthesized via the sol-gel method and sintered at three different temperatures (800˚C, 825˚C, and 850˚C), in order to evaluate the onset and completeness of the superconducting transition.

For all samples, the resistivity gradually decreased as the temperature was lowered, with a clear superconducting transition observed. The critical temperatures were determined based on the onset of the transition ($T_{c(onset)}$) and the temperature at which the resistivity dropped to zero ($T_{c(offset)}$). The width of the transition ($\Delta T_c = T_{c(onset)} - T_{c(offset)}$) was also calculated to assess the homogeneity and quality of the superconducting phase in each sample.

As shown in Fig. 5, the temperature-dependent resistivity (ρ–T) curves illustrate the superconducting transition behavior of $HgBa_2Ca_2Cu_3O_{8+\delta}$ samples sintered at different temperatures (800, 825, and 850˚C). All samples exhibit a similar $T_{c(onset)}$ of approximately 171.3 K; however, the curve shape and the transition width (ΔT_c) vary notably with the sintering temperature [31]. For the sample sintered at 800˚C, the resistivity starts to decrease at a high temperature, but the transition is relatively broad ($\Delta T_c \approx 17$ K) until reaching $T_{c(offset)} \approx 127$ K, indicating weak grain connectivity and incomplete formation of the superconducting phase, along with the possible presence of secondary phases that increase resistivity in the pseudo-superconducting region [32]. Increasing the sintering temperature to 825˚C results in a steeper drop in resistivity within the transition region, narrowing ΔT_c to approximately 18.5 K and achieving $T_{c(offset)} \approx 131$ K, which reflects improved grain growth and enhanced structural homogeneity due to the greater thermal energy available during synthesis. At 850˚C, the curve exhibits the sharpest transition with the narrowest $\Delta T_c \approx 18.3$ K and $T_{c(offset)} \approx 134$ K, indicating the formation of a high-purity Hg-1223 superconducting phase with strong intergranular connectivity and a homogeneous microstructure, despite approaching the upper sintering limit where excessive grain growth or the formation of undesirable secondary phases may occur [33].

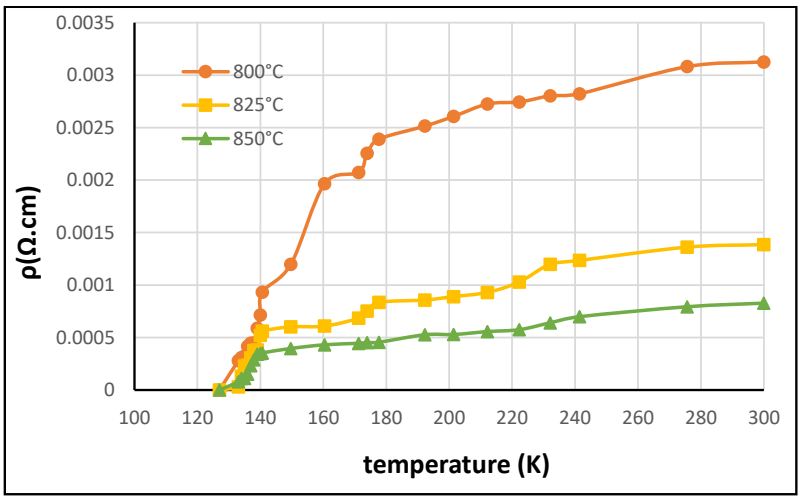

Fig. 5. Temperature-dependent resistivity curves for $HgBa_2Ca_2Cu_3O_{8+\delta}$ samples sintered at different temperatures (800, 825, and 850°C).

In conclusion, the electrical resistivity results demonstrate a progressive improvement in superconducting properties with increasing sintering temperature. The sample sintered at 850˚C exhibited the best performance in terms of sharp transition and homogeneity, making it the most promising candidate among the three.

Table 2. Superconducting transition temperatures and energy gap values for sol-gel prepared samples at different sintering temperatures.

Sample Temp (˚C)	$T_{c(onset)}$ (K)	$T_{c(offset)}$ (K)	ΔT_c (K)	Energy Gap (eV)
800	144	127.0	17.0	≈ 0.026
825	149.5	131.0	18.5	≈ 0.026
850	152.3	134.0	18.3	≈ 0.026

Summary and Analysis

The data presented in Table 2 illustrate a clear trend in the superconducting behaviour of the sol-gel prepared samples as the sintering temperature increases. All three samples exhibit the same onset critical temperature ($T_{c(onset)} \approx 171.3$ K), indicating that the formation of the superconducting phase initiates at a consistent temperature across all conditions [34]. However, the offset temperature ($T_{c(offset)}$) progressively rises from 127 K to 134 K as the sintering temperature increases from 800°C to 850°C, resulting in a gradual narrowing of the transition width (ΔT_c), from 44.3 K to 37.3 K.

This narrowing of ΔT_c suggests improved phase purity, enhanced grain connectivity, and better homogeneity at higher sintering temperatures. The energy gap remains approximately constant (≈ 0.026 eV) for all samples, supporting the conclusion that the superconducting phase is present in all cases, but with varying degrees of structural perfection [35].

Among the three, the sample sintered at 850°C demonstrated the sharpest transition and most uniform structure, implying superior superconducting performance. However, care must be taken at this temperature range, as it approaches the limit beyond which structural degradation or secondary phase formation may occur [36,37].

CONCLUSION

In this study, superconducting samples of the compound $HgBa_2Ca_2Cu_3O_{8+\delta}$ (Hg-1223) were successfully synthesized using the sol-gel method and sintered at three different temperatures: 800°C, 825°C, and 850°C. Structural, microstructural, and electrical characterizations were performed to evaluate the influence of sintering temperature on phase formation, grain morphology, and superconducting behavior. XRD analysis confirmed the formation of the Hg-1223 superconducting phase in all samples, with varying proportions depending on the sintering temperature. The sample sintered at 800°C exhibited the highest phase purity, while higher sintering temperatures led to improved crystallinity but also introduced minor secondary phases. Changes in lattice parameters and unit cell volume across the samples indicated subtle structural evolution due to temperature.

SEM images taken at a magnification of 5 μm revealed progressive grain growth, increased density, and enhanced grain connectivity with increasing sintering temperature. The sample sintered at 850°C displayed the most compact and homogeneous microstructure with minimal porosity and well-defined grain boundaries, suggesting more effective sintering conditions. Electrical resistivity measurements showed that all samples exhibited superconducting transitions starting around 171.3 K. However, the transition width (ΔT_c) decreased with increasing sintering temperature, indicating improved structural homogeneity. The sample sintered at 850°C demonstrated the sharpest transition ($\Delta T_c \approx 37.3$ K) and the best superconducting behavior among the three, although this temperature approaches the limit where structural degradation or unwanted secondary phases may appear. Overall, the results indicate that the sol-gel method is an effective route for synthesizing high-temperature superconductors of the Hg-based family. Among the studied sintering conditions, 850°C offered the best balance between phase formation, microstructural quality, and superconducting performance. These findings provide a strong foundation for further optimization of processing parameters and potential development of Hg-1223-based materials for superconducting applications.

ACKNOWLEDGEMENTS

This work was supported by the use of equipment from the Superconducting Graduate Laboratory in the Department of Physics, College of Education for Pure Sciences, University of Baghdad.

REFERENCES

1. J. G. Bednorz and K. A. Moller, Rev. Mod. Phys., 60, 585 (1988).
2. H. Mazaki, T. Ishida and T. Sakuma, Jpn. J. Appl. Phys., 27, 811 (1988).
3. L. B. Boldyreva, Int. J. Phys., 4, 26 (2016).
4. W. Meissner and R. Ochsenfeld, Naturwissenschaften, 21, 787 (1933).
5. A. H. Shaban, L. A. Mohammed, H. S. Hussein and K. A. Jasim, Dig. J. Nanomater. Biostruct., 17, 519 (2022).
6. A. M. Morales Rivera, J. A. Gómez Cuaspud, C. A. ParraVárgas and M. H. Brijaldo Ramirez, J. Supercond. Nov.Magn., 29, 1163 (2016).

7. Jasim, K.A., The effect of cadmium substitution on the superconducting properties of Tl1-x Cd x Ba2Ca2Cu 3O9-δ compound, Journal of Superconductivity and Novel Magnetism, 2013, 26(3), pp. 549–552.
8. A. Kareiva, J. Barkauskas, S. Mathur, Oxygen content and superconducting properties of Hg-based superconductors synthesized by sol–gel method, Journal of Physics and Chemistry of Solids, Volume 61, Issue 5, May 2000, Pages 789-797.
9. Hamadneh, I., Kuan, Y. W., Hui, L. T., & Abd-Shukor, R. (2006). undefined. Materials Letters, 60(6), 734-736. https://doi.org/10.1016/j.matlet.2005.10.002
10. Ahmed, B.A., Mohammed, J.S., Fadhil, R.N., ...Shaban, A.H., Al Dulaimi, A.H., The dependence of the energy density states on the substitution of chemical elements in the Se_6 $Te_{4-x}Sb_x$ thin film, Chalcogenide Letters, 2022, 19(4), pp. 301–308.
11. Kadhim, B.B., Khaleel, I.H., Hussein, B.H., ...Al-Maiyaly, B.K.H., Mahdi, S.H., Effect of gamma irradiation on the TlBa2Ca2Cu3O9-δ superconducting properties, AIP Conference Proceedings, 2018, 1968, 030054.
12. K. A. Jasim, R. Abd A. Fadil, K. M. Wadi and A. H. Shaban, Korean J. Mater. Res., 33, 9 (2023).
13. Abdulateef, A.N., Alsudani, A., Chillab, R.K., Jasim, K.A., Shaban, A.H., Calculating the mechanisms of electrical conductivity and energy density of states for $Se_8$5$Te_{10}Sn_{5-x}In_x$ glasses materials, *Journal of Green Engineering, 2020, 10(9), pp. 5487–5503*.
14. Aleabi, S.H., Watan, A.W., Salman, E.M.-T., kareem Jasim A.,Shaban, A.H., Alsaadi, T.M., The study effect of weight fraction on thermal and electrical conductivity for unsaturated polyester composite alone and hybrid, AIP Conference Proceedings, 2018, 1968, 020019.
15. Alwan, A. M., Ahmed, D. S., Saleman, U. N., & Ahmed, I. S. (2008). Effect of the peak phase delay on an acousto–optic interaction. Journal of Al-Nahrain University Science, 11(3), 89-97. https://doi.org/10.22401/jnus.11.3.11
16. A. J. Haider, R. H. Al-Anbari, G. R. Kadhim, and C. T. Salame, "Exploring potential environmental applications of TiO_2 nanoparticles," Energy Procedia 119, 332–345 (2017).
17. Tokiwa, K., Ito, S., Okumoto, H., Mikusu, S., Iyo, A., Tanaka, Y., & Watababe, T. (2003). Journal of Low Temperature Physics, 131(3/4), 637-641. https://doi.org/10.1023/a:1022992412312
18. Jasim, K.A., Alwan, T.J., Effect of Oxygen Treatment on the Structural and Electrical Properties of $Tl_{0.85}Cd_{0.15}Sr_2CuO_{5-\delta}$,$Tl_{0.85}Cd_{0.15}Sr_2Ca_2Cu_2$ O $_{7-\delta}$ and $Tl_{0.85}Cd_{0.15}Sr_3Ca_2Cu_3$ O $_{9-\delta}$ Superconductors, Journal of Superconductivity and Novel Magnetism, 2017, 30(12), pp. 3451–3457.
19. Omar, B.A., Fathi, S.J., Jassim, K.A., Effect of Zn on the structural and electrical properties of high temperature HgBa2Ca2Cu3O8+δ superconductor, AIP Conference Proceedings, 2018, 1968, 030047.
20. Wadi, K.M., Jasim, K.A., Shaban, A.H., Kamil, M.K., Nsaif, F.K., The effects of sustainable manufacturing pressure on the structural properties of the pb2ba2ca2cu3o9+σ compound, Journal of Green Engineering, 2020, 10(9), pp. 6052–6062.
21. D. Zhang, C. Boffo and C. David. Dunand, Nat. Commun., 16, 1933 (2025).
22. Jasim, K.A., Makki, S.A., Almohsin, A.A. Comparison study of transition temperature between the superconducting compounds Tl0.9Pb0.1Ba2Ca2Cu3O9, Tl0.9Sb0.1Ba2Ca2Cu3O9-δ and Tl0.9Cr0.1Ba2Ca2Cu3O9-δ, Physics Procedia, 2014, 55, pp. 336–341.
23. L. A. Mohammed, H. S. Hussein, H. M. J. Haider, K. A. Jasim, H. Shaban, S. G. M. Askar and F. W. Ali, AIP Conf. Proc., 2190, 020018 (2019).
24. Jasim, K.A., Mohammed, L.A., The partial substitution of copper with nickel oxide on the Structural and electrical properties of $HgBa_2$ Ca_2 $Cu_{3x}Ni_x$ $O_{8+\delta}$ superconducting compound, Journal of Physics: Conference Series, 2018, 1003(1), 012071.
25. S. D. Peacor, R. A. Richardson, J. Burm, C. Uher and A. B. Kaiser, Phys. Rev. B, 42, 2684 (1990).
26. J. Kawashima, Y. Yamada and I. Hirabayashi, Physica C, 306, 114 (1998).
27. *Watan, A.W., Aleabi, S.H., Risan, R.H., Jasim, K.A., Shaban, A.H., Preparation and Physical Properties of Doped* $CdBa_{2-x}$ $Sr_xCa_2Cu_3O_{8+\delta}$ *Compound, Energy Procedia, 2017, 119, pp. 466–472*
28. G. C. Che, Y. K. Du, F. Wu and Z. X. Zhao Solid State Commun., 89, 903 (1994).
29. Al-Khafaji, R.S.A., Jasim, K.A., Dependence the microstructure specifications of earth metal lanthanum La substituted Bi2Ba2CaCu2–XLaXO8+δon cation vacancies, AIMS Materials Science, 2021, 8(4), pp. 550–559.
30. A. Jabbar, M. Mumtaz and K. Nadeem, Eur. Phys. J. Appl. Phys., 69, 30601 (2015).
31. L. Ganapathi, A. Kumar and J. Narayan, Physica C, 167, 669 (1990).
32. I. Hamadeh, Y. W. Kuan, L. T. Hui and R. Abd-Shukor, Mater. Lett., 60, 734 (2006).
33. Fathi, S. J. (2025, February). Influence of substitution on structural and electrical properties of $Bi_xBa_2Ca_2Cu_3O_{10+\delta}$ superconductor. Paper presented at TMREES25Ma International Conference, Casablanca, Morocco. Journal of Physics: Conference Series, IOP Publishing.

34. Tian W, Shao H M, Zhu J S andWang Y N ,"Physica Status Solidi" (2006). (2006). physica status solidi (a), 203(11). https://doi.org/10.1002/pssa.v203:11
35. Collins, M. (2000). Research: An introduction to principles, methods and practice. Evaluation and Program Planning, 23(4), 472-473. https://doi.org/10.1016/s0149-7189(00)00038-0
36. Biju, A., Syamaprasad, U., Rao, A., Xu, J., Sivakumar, K., & Kuo, Y. (2007). Structural and transport properties of ND doped (bi,pb)-2212. Physica C: Superconductivity, 466(1-2), 69-75. https://doi.org/10.1016/j.physc.2007.06.013
37. Fathi, S. J., & Jasim, K. A. (2024). Investigation into structural and electrical characteristics of the Hg.Ag,$Ba_2Ca_2Cu_3O_8$+δ superconductor. EURACA, Decree 818559064 – France.